UV Photodesorption of Novel Molecular Beam Induced NO Layers on NiO(111)/Ni(111)

B. D. Zion and S. J. Sibener*

The James Franck Institute and Department of Chemistry, The University of Chicago, Gordon Center for Integrative Science, 929 East 57th Street, Chicago, Illinois 60637

Received: December 10, 2007; In Final Form: February 6, 2008

The photodesorption and photoreactivity of the molecular beam dosed NO/NiO(111)/Ni(111) system has been examined using high-resolution electron energy loss spectroscopy (HREELS). The molecular beam dosed surface exhibits three major vibrational peaks, which we attribute to a linear bonding NO species at 230 meV, a bent bonding NO species at 197 meV, and a stretching mode of NO_2 at 160 meV. UV photon irradiation causes the attenuation of these peaks accompanied by simultaneous emergence of a fourth vibrational peak at 215 meV. The emergence of this peak is explained by a mechanism of selective desorption of the original, linear-bound NO species and a reaccommodation of the beam-induced, bent NO structure to a new state on the lower coverage surface. The measured desorption cross sections and wavelength dependence are consistent with those of other studies of photochemical processes on such interfaces, indicating that photoinduced electron transfer from the substrate to the adsorbate is the mechanism responsible for the observed behavior.

Introduction

The band structure of NiO makes it an interesting surface on which to study photoreactivity, and it has been the subject of calculational and empirical studies.[1−4] Reflectance spectrum studies have shown that the optical absorption coefficient is vanishingly small from 0 to 4 eV, where it has a sharp edge. This optical absorption cutoff corresponds to 300 nm, and the first optical absorption peak corresponds to 288 nm. The peak structure of the optical absorption coefficient is broadly defined on top of a smoothly sloping background.[4]

In this article, we will focus on the properties of NO desorption and photoreactivity on the NiO surface. We show that exposing the NO/NiO(111)/Ni(111) surface to UV light results in dramatic changes in the vibrational signature as monitored by high-resolution electron energy loss spectroscopy (HREELS). The three previously observed peaks[5] for the nonirradiated system attenuate while a fourth, new peak emerges. In light of previous studies of the NO/NiO system under UV irradiation, these changes are explained by a selective desorption of the linearly bound NO surface species leaving a predominance of bent NO adsorbates. The bent NO reaccommodates to the depleted surface environment, resulting in the emergence of the new vibrational peak.

Many studies have been carried out on the photoreactivity of the NO covered NiO surface[6−9] with the majority of the studies focusing on the NiO(100) surface.[10−15] There are also a number of studies examining the differences between photodesorption from the (100) and (111) NiO surfaces.[16−21]

Briefly, the observed behavior for UV laser desorption of NO from NiO(100) is a nonthermal vibrational population, a bimodal velocity distribution, and a rotational state dependence in the higher velocity channel.[14] The proposed desorption mechanism is the Antoniewicz variation of the MGR model where an NO^- ion is temporarily created by charge transfer from the substrate to the adsorbate. The transient ion has a bonding geometry normal to the surface, a bond distance closer to the surface than the un-ionized adsorbate, and a bond length shorter than the free molecule. Thus, when the adsorbate, which has a bonding geometry tilted to the surface by 45°, is transformed to its temporary negative ion state, it accommodates to the surface by straightening upright and moving closer to the surface. When the electron transfers back to the substrate, the ground state molecule finds itself too close to the NiO surface, high on the repulsive part of the potential energy surface, with rotational energy acquired from untilting its bond geometry and with an intermolecular bond distance that is too short. The longer the transient state exists, the higher on the repulsive part of the potential energy surface the molecule is and the more rotational energy the molecule has when released. This similtaneous deformation of bond distance and bond angle gives rise to the rotational-translational energy coupling, while the ionic bond length gives rise to the nonthermal vibrational temperature observed.[11,13,14] Desorption cross sections were measured as 1.9×10^{-17} cm^2 at 314 nm;[14] 7×10^{-17} cm^2 at 193 nm;[21] and 6×10^{-17} cm^2 at 194 nm.[17] There is one measurement of a NO_2 UV photodesorption cross section from NiO(100) which is reported as 3×10^{-19} cm^2 at 193 nm.[21]

Similar observations have been made for NO UV photodesorption from NiO(111). Three major differences are found for desorption from the (111) surface: the lower translational energy channel is the dominant velocity, there is no rotational-translational energy coupling, and there is a spin state dependence of the vibrational temperature. The $^2\Pi_{3/2}$ state has a vibrational temperature of 2050 K and the state $^2\Pi_{1/2}$ has a vibrational temperature of 1600 K, whereas for desorption from the NiO(100) surface the vibrational temperature is 1850 K, independent of the spin state. This discrepancy can be explained by the different magnetic properties of the two surfaces of antiferromagnetic NiO. On the (100) surface lattice, the anit-parallel spin orientations have no overall spin. However, for the (111) surface, the spins show a preferential orientation resulting in a dependence on the electron spin for the recom-

* To whom correspondence should be addressed. E-mail: s-sibener@uchicago.edu.

10.1021/jp711629s CCC: $40.75
Published on Web 03/27/2008

bination probability of the transient NO^- state.[17,19,20] Desorption cross sections for the NO/NiO(111) system were measured as 1.4×10^{-17} cm^2 at 193 nm;[21] 6×10^{-17} cm^2 at 193 nm; 3×10^{-17} cm^2 at 248 nm; and 3.5×10^{-18} cm^2 at 354 nm.[17]

Experimental Section

The experiments were conducted in a two level ultrahigh vacuum (UHV) scattering chamber with a connected molecular beam line described previously.[5] Briefly, the UHV chamber, with a base pressure of 1×10^{-10} Torr, is equipped with low-energy electron diffraction (LEED), Auger electron spectroscopy (AES), an ion gun, an effusive doser on the upper level for surface preparation and characterization, a high-resolution electron energy loss (HREEL) spectrometer, a residual gas analyzer (RGA), external ports for introducing a molecular beam for dosing, and a UV light for photodesorption on the lower level.

The sample used for the present work is a nickel single crystal, cut and polished to within 0.2° of the close-packed (111) plane. The Ni sample, affixed to a temperature controlled mount, is cleaned by repeated cycles of argon ion sputtering at a backing pressure of 5×10^{-5} Torr, and annealing at 1100 K until AES shows a clean surface. The clean sample has a very sharp LEED pattern with 6-fold symmetry. Further treatment of the clean surface to prepare a NiO(111) surface is done by exposing the sample to 1×10^{-7} Torr of O_2 for 15 min to 1 h followed by annealing to 600 K for 10 min. The thin oxide surface exhibits diffuse LEED spots with 6-fold symmetry with spots slightly closer together in reciprocal space than the clean Ni(111) due to the relatively larger lattice constant in real space. The AES shows oxygen and nickel signals that are nearly equal in peak-to-peak height. This surface is retreated between experiments by annealing to 600 K for 10 min.

The substrate was cooled to a base temperature of 110 K before NO exposure. The preparation of the overlayer was achieved by 60 min dosing with a weakly supersonic NO beam characterized by a mean kinetic energy of ~75 meV with a fwhm resolution of ~60 meV. The UV photodesorption experiments were conducted by exposing the prepared overlayer to light from a HgXe arc lamp and grating monochromator (Oriel), with ~20 nm fwhm. The power delivered to the surface was wavelength-dependent: for 306 nm irradiation, 5.0 mW cm^{-2} was used; for 403 nm, 2.2 mW cm^{-2}; for 575 nm, 1.9 mW cm^{-2}. Photon dosing times ranged from 5 s for the highest power and shortest wavelength to 90 min for the lowest power and longest wavelength radiation. The time required for HREELS data collection ranged for 5 min to 1 h. HREELS data were collected alternately with photon irradiation of the surface.

Results

Figure 1 shows a series of HREEL spectra of the NO/NiO-(111) system after sequential photon irradiation with 306 nm light. In these spectra, a peak at ~215 meV is just barely discernible as a shoulder of the NO stretch peak at 230 meV on the NO-dosed, nonirradiated surface. This 215 meV peak grows in intensity with increasing photon dose until it dominates the vibrational spectrum. The curve fits in this figure differ from the curve fits of the nonirradiated system in that an additional Gaussian is added to account for the photoinduced peak. Figure 2 shows the same data as in Figure 1 but with background subtracted, and the various components of the curve fit that comprise the different vibrational frequencies, including the NiO phonons, are shown. Figure 3 shows the peak heights for the various vibrations due to NO adsorbates. The new feature emerges after 3×10^{17} photons cm^{-2} of 306 nm irradiation. The curves are exponential decays fit to the attenuation of the three principle vibrations as a function of photon dose. Similar HREELS data are collected for irradiation of the NO/NiO(111) surface with 403 and 575 nm light, and the vibrational peaks are analyzed in the same way as the data for the spectra collected after 306 nm irradiation. Figure 4 shows a side by side comparison of the intensity of each vibrational feature as a function of photon dose for each of the three wavelengths.

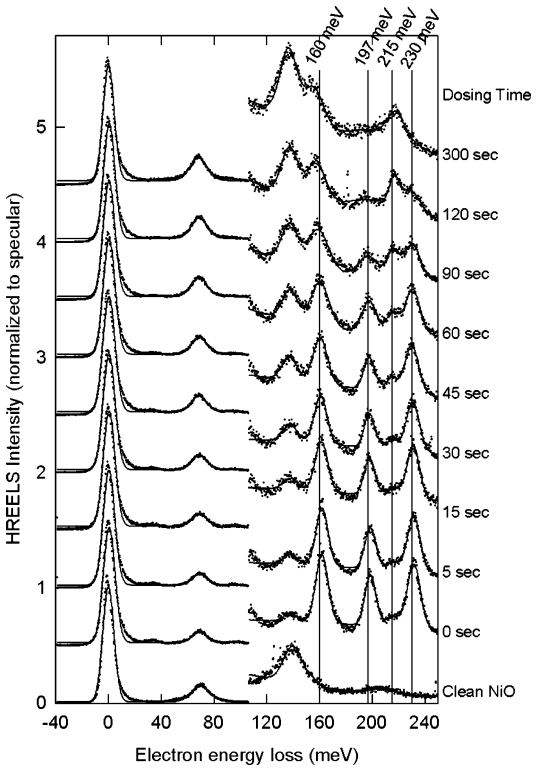

Figure 1. Series of HREEL spectra recorded after sequential exposure of the NO/NiO(111) system to 306 nm irradiation. The data are fit with a curve consisting of eight Gaussians, an exponential decay, and a constant background. The eight Gaussians are used to account for the elastic reflection, three NiO phonons, and vibrational peaks at 160, 197, 215, and 230 meV. It is clear by inspection that the three main vibrational peaks present at 160, 197, and 230 meV attenuate under photon exposure while the 215 meV peak grows.

Discussion

Most apparent in the HREEL spectra is the emergence of a new vibrational peak induced by a UV photoreaction. Two possibilities for the genesis of the new peak are (i) chemical reaction or (ii) structural reaccommodation of existing species. While we cannot definitively exclude chemical reaction as the explanation of our data, the creation of a new chemical species with the appropriate vibrational signature from the surface reagents available is improbable.[10,22−24] We therefore limit our discussion to surface rearrangement of existing species induced by photoinitiated processes. As illustrated in Figure 5, the 230 and 197 meV vibrational peaks can be assigned to the linear NO^+ and bent NO^- surface species, respectively. Considering the organometallic compound, $[RuCl(NO)_2(P(C_6H_5)_3)_2]^+$, where the two different NO ligands are found, the measured vibrational energies are 229 and 208 meV for the linear and bent species, respectively.[25] That 208 meV peak is close to the observed energy of the new vibrational energy at 215 meV induced by

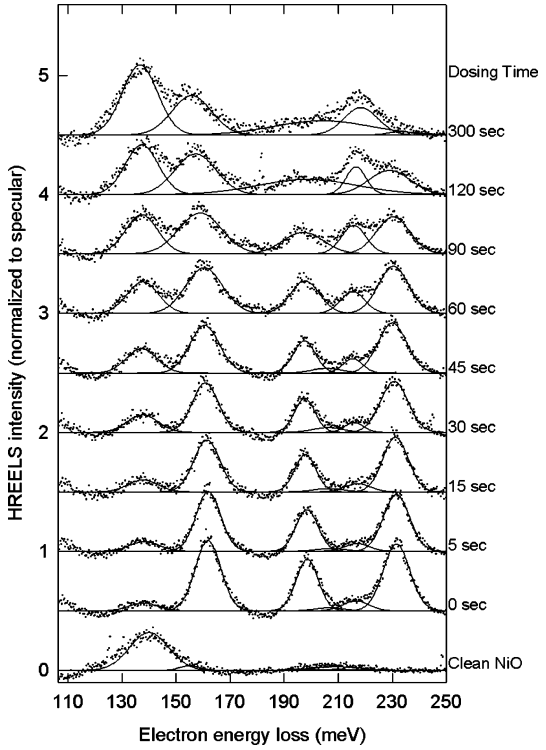

Figure 2. Same data from Figure 1 with background subtracted. Individual components of the total curve fit are shown. For small signals that are on the order of the noise in the data, it is difficult to obtain a meaningful fit to the data. For larger signals, the curve fits give useful, quantitative data.

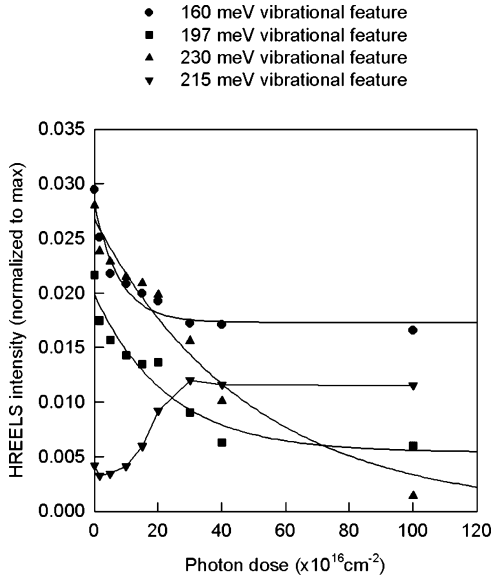

Figure 3. Peak heights for the various vibrational features as a function of photon exposure at 306 nm. The attenuation of the three main vibrational features are fit with exponential decay curves to extract desorption cross sections. The line connecting the points representing the new 215 meV vibrational feature is a guide to the eye. The 215 meV grows in with photon dose to a maximum at $\sim 3 \times 10^{17}$ photon cm^{-2}.

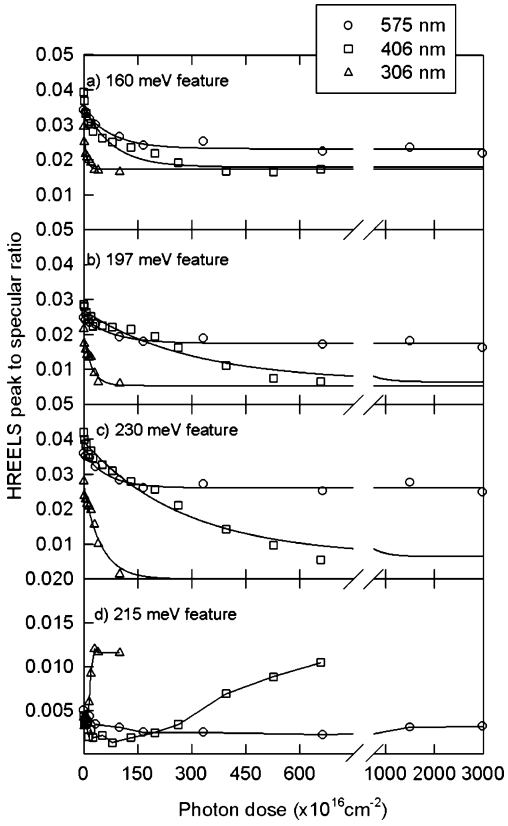

Figure 4. Compilation of all of the photo desorption data and exponential decay curve fits. The line connecting the points representing the new 215 meV vibrational feature is a guide to the eye. Each vibrational peak is compared to data for the three wavelengths of light used in this experiment. The increasing efficacy of the photodesorption in the top three panels and the photoreactivity in the bottom panel as a function of shortening wavelength can clearly be seen.

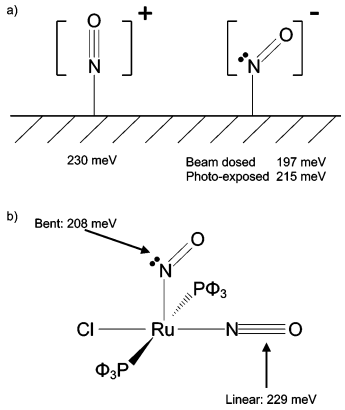

Figure 5. (a) Schematic representation of the proposed bonding geometries for the linear NO^+ and the bent NO^- species. The two bonding geometries and their respective vibrational assignments are shown. For the bent configuration, the first number given is the observed vibrational energy upon NO molecular beam dosing while the second number is the value measured after photon irradiation of the NO dosed surface. (b) Molecular configuration of the model compound $[RuCl(NO)_2(P(C_6H_5)_3)_2]^+$. The vibrational frequencies and assignments of the linear and bent NO ligands are from ref 25, while the molecular graphic is closely modeled after ref 26.

photon irradiation. Thus, we propose that the observed result is caused by a selective desorption of the linearly bound NO^+ species. The hitherto sterically hindered NO^- species on the highly adsorbate covered surface accommodates to the newly depopulated surface, allowing a relaxation of bonding geometry. This new structure may well resemble the organometallic molecule in both geometry and vibrational energy. Thus, the final state reflects not a chemical reaction at the surface but a selective desorption leaving a novel surface overlayer different from both the high-coverage molecular beam dosed surface and the low-coverage backfill dosed surfaces.

TABLE 1: Desorption Cross Sections Determined by Fitting the Peak Signal Attenuation vs Photon Dose Curves with Exponential Decay Curves

	vibrational feature		
wavelength	160 meV	197 meV	229 meV
306 nm	1.3×10^{-17} cm^2	4.4×10^{-18} cm^2	2.1×10^{-18} cm^2
403 nm	1.3×10^{-18} cm^2	3.4×10^{-19} cm^2	3.6×10^{-19} cm^2

TABLE 2: Desorption Cross Sections from the Literature

system	wavelength	cross section	reference
NO/NiO(100)	193 nm	7×10^{-17} cm^2	21
	194 nm	6×10^{-17} cm^2	17
	314 nm	1.9×10^{-17} cm^2	14
NO_2/NiO(100)	193 nm	3×10^{-19} cm^2	21
NO/NiO(111)	193 nm	1.4×10^{-17} cm^2	21
	193 nm	6×10^{-17} cm^2	17
	248 nm	3×10^{-17} cm^2	17
	354 nm	3.5×10^{-18} cm^2	17

The cross sections from photodesorption measurements are tabulated in Table 1 and are comparable to previous results, tabulated in Table 2. The variation in decay with wavelength matches previous results of other authors and is in good theoretical agreement with the model of band gap excitation of electrons. The most energetic photons, 306 nm, being near the band edge, give high values for cross sections, whereas the lower energy UV irradiation, 403 nm, is further from the band edge and shows lower cross sections. The lowest energy wavelength, 575 nm, does not give meaningful quantitative results for cross sections using an exponential decay, because the photon-independent, spontaneous (and very slow) decay in the vibrational signal as a function of time overwhelms the photoinduced desorption. The lack of photoreaction at this wavelength can be seen clearly in Figure 4c and 4d where a significant portion of the 230 meV peak is retained and very little of the 215 meV peak is created after extended photon dosing, implying that the desorption cross section at this long wavelength is marginal, perhaps even zero. We do find that the energy dependence is in good agreement with the model of desorption induced by electron transfer.

The results of these experiements are that a new vibrational peak emerges after UV photoirradiation of the molecular beam dosed NO/NiO(111)/Ni(111) system. We feel that the most probable scenario is a selective desorption of the linear NO^+ surface state followed by relaxation of the bent NO^- species on the depleted surface. The UV desorption cross sections obtained are in agreement with previous studies conducted on the lower coverage NO/NiO system and show the same wavelength dependence. The same desorption induced by the electron-transfer mechanism previously proposed for the lower coverage systems is responsible for the observed data. In closing, we note that follow-on, future refinement of the photodesorption and restructuring mechanisms herein discussed could be accomplished by using a more finely tuned light source to explore desorption thresholds coupled with mass, angle, and kinetic energy resolved studies of the desorbing species with simultaneous scanning tunneling microscopy (STM) imaging of *in situ* structural change.

Summary

We have used UV irradiation from a monochromated HgXe lamp to expose a NO/NiO(111)/Ni(111) surface to quantified doses of wavelength-selected photons, leading to notable structural changes in the overlayer. Examination of the resultant vibrational signature by HREELS reveals dramatic changes in surface species upon UV irradiation. Such irradiation causes the three previously observed vibrational peaks, linear NO^+ stretch at 230 meV, bent NO^- stretch at 197 meV, and NO_2 stretch at 160 meV, for the nonirradiated system to attenuate while a fourth, new peak at 215 meV emerges. These changes are explained by a selective desorption mechanism in which the linearly bound NO^+ surface species is preferentially desorbed and the remaining NO^- adsorbate reaccommodates to the depleted surface. The resulting structural adjustment is observed as the emergence of the new vibrational feature. The measured cross sections and wavelength dependencies are consistent with photo-initiated desorption induced by electron transfer involving the substrate and the overlayer.

Acknowledgment. This work was supported by the Air Force Office of Scientific Research and the Chemical Sciences, Geosciences and Biosciences Division, Office of Basic Energy Sciences, Office of Science, U.S. Department of Energy, Grant DE-FG02-00ER15089. We also acknowledge supplemental infrastructure support from the NSF-Materials Research Science and Engineering Center at the University of Chicago, NSF-DMR-0213745.

References and Notes

(1) Kunz, A. B. *J. Phys. C: Solid State Phys.* **1981**, *14*, L455−L460.

(2) Hugel, J.; Carabatos, C. *J. Phys. C: Solid State Phys.* **1983**, *16*, 6713−6721.

(3) Hugel, J.; Carabatos, C. *J. Phys. C: Solid State Phys.* **1983**, *16*, 6723−6730.

(4) Powell, R. J.; Spicer, W. E. *Phys. Rev. B* **1970**, *2*, 2182−2193.

(5) Zion, B. D.; Sibener, S. J. *J. Chem. Phys.* **2007**, *127*, 154720.

(6) Ferm, P. M.; Budde, F.; Hamza, A. V.; Jakubith, S.; Weide, D.; Andresen, P.; Freund, H.-J. *Surf. Sci.* **1989**, *218*, 467−493.

(7) Yoshinobu, J.; Guo, X.; Yates, J. T., Jr. *J. Vac. Sci. Technol., A* **1991**, *9*, 1726−1731.

(8) Yoshinobu, J.; Guo, X.; Yates, J. T., Jr. *J. Chem. Phys.* **1990**, *92*, 7700−7707.

(9) Thiel, S.; Klüner, T.; Freund, H.-J. *Chem. Phys.* **1998**, *236*, 263−276.

(10) Mull, T.; Menges, M.; Baumeister, B.; Odörfer, G.; Geisler, H.; Illing, G.; Jaeger, R. M.; Kuhlenbeck, H.; Freund, H.-J.; Weide, D.; Schüller, U.; Andresen, P.; Budde, F.; Ferm, P.; Hamza, V.; Ertl, G. *Phys. Scr.* **1990**, *41*, 134−139.

(11) Klüner, T.; Freund, H.-J.; Freitag, J.; Staemmler, V. *J. Mol. Catal. A: Chem.* **1997**, *119*, 155−163.

(12) Eichhorn, G.; Richter, M.; Al-Shamery, K.; Zacharias, H. *Surf. Sci.* **1996**, *368*, 67−70.

(13) Klüner, T.; Thiel, S.; Freund, H.-J.; Staemmler, V. *Chem. Phys. Lett.* **1998**, *294*, 413−418.

(14) Eichhorn, G.; Richter, M.; Al-Shamery, K.; Zacharias, H. *J. Chem. Phys.* **1999**, *111*, 386−397.

(15) Zacharias, H.; Eichhorn, G.; Schliesing, R.; Al-Shamery, K. *Appl. Phys. B* **1999**, *68*, 605−609.

(16) Cappus, D.; Menges, M.; Xu, C.; Ehrlich, D.; Dillmann, B.; Ventrice, C. A.; Libuda, J.; Bäumer, M.; Wohlrab, S.; Winkelmann, F.; Kuhlenbeck, H.; Freund, H.-J. *J. Electron Spectrosc. Relat. Phenom.* **1994**, *68*, 347−355.

(17) Menges, M.; Baumeister, B.; Al-Shamery, K.; Freund, H.-J.; Fischer, C.; Andresen, P. *J. Chem. Phys.* **1994**, *101*, 3318−3325.

(18) Baumeister, B.; Freund, H.-J. *J. Phys. Chem.* **1994**, *98*, 11962−11968.

(19) Al-Shamery, K.; Menges, M.; Beauport, I.; Baumeister, B.; Klüner, T.; Mull, T.; Freund, H.-J.; Fischer, C.; Andresen, P.; Freitag, J.; Staemmler, V. In *Proceedings of the International Soceity of Optical Engineering/Laser Conference*, Los Angeles, CA, 1994; Dai, H.-L., Sibener, S. J., Eds.; pp 182−191, v 2125.

(20) Al-Shamery, K. *Appl. Phys. A* **1996**, *63*, 509−521.
(21) Mull, T.; Kuhlenbeck, H.; Odörfer, G.; Jaeger, R.; Xu, C.; Baumeister, B.; Menges, M.; Illing, G.; Freund, H.-J.; Weide, D.; Andresen, P. In *Desorption Induced by Electronic Transitions, DIET IV*; Betz, G., Varga, P., Eds.; Springer-Verlag: Berlin, 1990; Vol. 19, pp 169−173.
(22) Kuhlenbeck, H.; *Appl. Phys. A* **1994**, *59*, 469−477.
(23) Kuhlenbeck, H.; Odörfer, G.; Jaeger, R.; Illing, G.; Menges, M.; Mull, T.; Freund, H.-J.; Pöhlchen, M.; Staemmler, V.; Witzel, S.; Scharfschwerdt, C.; Wennemann, K.; Liedtke, T.; Neumann, M. *Phys. Rev. B* **1991**, *43*, 1969−1986.
(24) Schönnenbeck, M.; Cappus, D.; Klinkmann, J.; Freund, H.-J.; Petterson, L. G. M.; Bagus, P. S. *Surf. Sci.* **1996**, *347*, 337−345.
(25) Pierpont, C. G.; Derveer, D. G. V.; Durland, W.; Eisenberg, R. *J. Am. Chem. Soc.* **1970**, *92*, 4760−4762.
(26) Albert, M. R.; Yates, J. T. *The Surface Scientist's Guide to Organometallic Chemistry*; American Chemical Society: Washington, DC, 1987.